Surface Science 154 (1985) 22–34
North-Holland, Amsterdam

VELOCITY DEPENDENCE OF AZIMUTHAL ANISOTROPIES IN ION SCATTERING FROM RHODIUM {111}

Che-Chen CHANG, Lisa A. DeLOUISE *, Nicholas WINOGRAD and Barbara J. GARRISON **

Department of Chemistry, The Pennsylvania State University, University Park, Pennsylvania 16802, USA

Received 19 June 1984; accepted for publication 26 November 1984

The scattering of He^+, Ne^+ and Ar^+ ions from Rh {111} is measured as a function of the azimuthal angle of the primary ion for an incident polar angle of 70° from the surface normal and an inplane collection angle of 60°. In this case anisotropy is defined as the ratio of the yield of ions scattered having the azimuth of ⟨110⟩ to the yield of those having the azimuth of ⟨211⟩. The yield ratio for all particle types correlates with particle velocity. The ratio is ~1 at low velocities, decreases to ~0.2 at 8×10^6 cm/s and then increases to a value of 1.4 at 25×10^6 cm/s. Molecular dynamics calculations have been performed for Ne^+ ion scattering from Rh{111} in order to understand the changes in anisotropy with particle velocity. Qualitative agreement with the experimental results is obtained without having to account for neutralization. A neutralization probability that depends on the collision time improves the agreement between the calculated and experimental yield ratios. A velocity dependent probability will not affect the ratio of yields in two different azimuthal directions.

1. Introduction

The scattering of keV ions from solids has been used to determine both the elemental composition of the surface layer and the bonding geometry of adsorbed species [1]. The geometrical determinations are usually deduced by examining angular anisotropies in the ion scattering intensities. These anisotropies are then attributed to blocking, shadowing, multiple scattering, and focussing of the ion by surface atoms. Ideally one would like to interpret the scattered ion intensity using simple geometrical arguments and not have to resort to lengthy computer simulations. This goal is best accomplished if care is taken in choosing the experimental angles of incidence and collection [1d,1e]. However, these simple concepts have been used to make surface structure

* Present address: IBM Research Laboratory, San Jose, California 95193, USA.
** Camille and Henry Dreyfus Teacher–Scholar.

0039-6028/85/$03.30

determinations for less than ideal experimental geometries [1a,1c], even though recent investigations suggest that neutralization of the scattered ions may be a determining factor in controlling the nature of the azimuthal anisotropies [2,3]. It has even been possible to make quantitative comparisons between experiment and computer simulations for both neutrals [4] and ions [5]. These comparisons, although more sophisticated than the earlier ones, usually result in interpretations along fairly straightforward lines. A fundamental question regarding the use of these arguments in determining unknown surface structures still remains.

In this study, we test the application of these simple concepts by examining the scattering of noble gas ions at near grazing angles of incidence and collection from clean Rh{111}. In a similar study where Ne^+ ions at energies between 200 and 400 eV were scattered from Ni{111}, the scattered intensity when the ion bombarded along the ⟨110⟩ direction was larger than that along the ⟨211⟩ direction [6]. The investigators interpreted these results to indicate a surface channel in the ⟨110⟩ direction that can readily focus the ion beam in the inplane direction.

The results reported here suggest that such simple explanations of the ion scattering intensity are not always correct. We find for an incident polar angle of 70° and collection at 60°, both measured from the surface normal, that the azimuthal angle at which there is maximum intensity changes with primary ion type (He^+, Ne^+, or Ar^+). The change in anisotropy as measured by the ratio of the yield along the ⟨110⟩ azimuth to the yield along the ⟨211⟩ azimuth can be correlated to the incident particle velocity. The scattering is isotropic at low velocities. As the velocity increases the scattering is first greater in the ⟨211⟩ direction and then reverses and is greater along the ⟨110⟩ direction. This change in anisotropy is not easily explained without performing molecular dynamics calculations. These calculations predict the qualitative change in yield ratio as a function of velocity without correction for the neutralization probability of the scattered ions. The agreement between the calculated and measured yield ratio, however, can be improved by including a simple neutralization factor that depends on the time of collision, i.e., the time that the ion interacts with the surface. A neutralization probability that depends only on the final velocity does not alter the ratio of yields in the two different azimuthal directions.

2. Experimental

The angle-resolved ion scattering spectrometry (ISS) experiments were performed in a multitechnique ultra-high vacuum apparatus described previously [7]. The noble gas ion (He^+, Ne^+, or Ar^+) beam was generated by a differentially pumped Leybold Heraeus (LH) ion gun. The incident beam

energy was varied between 0.2 and 2.5 keV, maintaining a constant current of 1–10 nA focussed into a $\sim 2 \times 2$ mm spot. Under these conditions the system pressure typically remained $< 1 \times 10^{-9}$ Torr.

The LH-EA11 bipolar energy analyzer was used to detect the scattered ions in the plane of incidence. This analyzer images a slightly arched $\sim 1 \times 10$ mm sample area and is characterized by a $\pm 4°$ polar angle acceptance. For these experiments the spectrometer was operated in the constant transmission mode, with a retarding ratio of 4. These operation parameters insured that there was a constant acceptance angle at the sample during the kinetic energy sweep. Under these conditions the experimental scattering angle was fixed at $\theta_s = 50°$. The primary ion beam was incident on the surface at $\psi_{in} = 70°$ and the collection angle was $\psi_{ex} = 60°$. Both of these latter angles are measured from the surface normal as shown in fig. 1a.

The Rh{111} crystal was cleaned by cycles of high temperature annealing and oxygen dosing which is an established procedure for removing bulk carbon from Rh samples [7]. In addition, Ar^+ ion sputtering was used to reduce the levels of F, S, and Cl contamination. X-ray Photoelectron Spectroscopy (XPS), Secondary Ion Mass Spectrometry (SIMS), and ISS were used to judge the quality of crystal cleanliness. The clean sample exhibited a sharp (1×1) LEED pattern expected for the Rh{111} surface. The crystal was fastened onto a 2

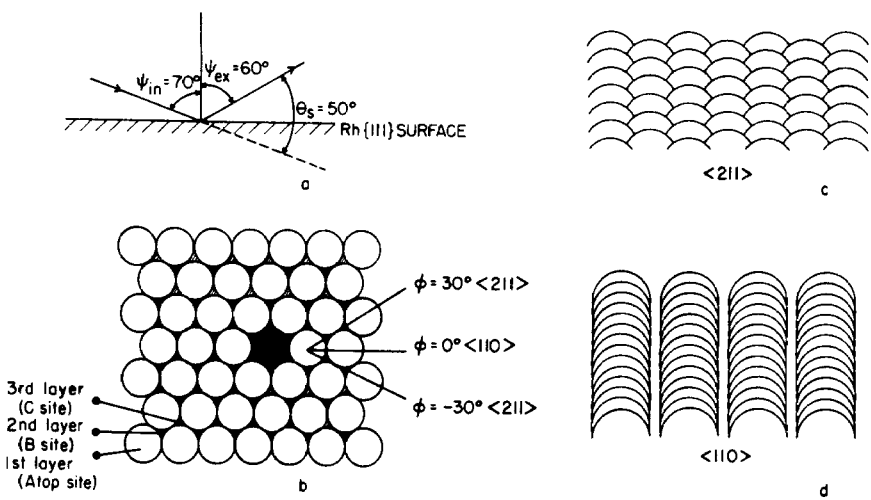

Fig. 1. Rhodium {111} geometries. (a) Experimental configuration and angles of the ISS system. (b) {111} crystal face showing the azimuthal directions and the impact zone for the calculations (darkened hexagon). (c) Rh{111} surface as viewed at a polar angle of 70° from the surface normal parallel to the ⟨211⟩ direction. (d) Rh{111} surface as viewed at a polar angle of 70° from the surface normal parallel to the ⟨110⟩ direction.

cm diameter Ta plate by two Ta clips [7]. This plate was mounted on a Thermionics precision manipulator equipped with 360° of rotation in the crystal plane, defined to ±1°. Due to the glancing geometry of the experimental setup the Ta clips prevented full 360° azimuthal scans. Considerable care was taken to prevent the beam from significantly damaging the structure of the crystal surface. A flag normally blocked the beam from interacting with a freshly annealed crystal. To measure a scattered ion intensity at a given azimuthal angle, the flag was removed for about 10 s while the signal was counted at the appropriate kinetic energy. This procedure was repeated at non-sequential azimuthal angles to generate the entire angular scan. After the last experimental point was recorded, the intensity measurement at the initial angle was repeated to be sure that any beam induced crystal damage did not influence the experimental results.

3. Description of the calculation

A classical dynamics procedure was employed to simulate the ion scattering process. This procedure consists of utilizing a microcrystallite of Rh atoms with the {111} crystal face exposed. The primary particle is allowed to impinge at a specific incident polar angle along a given azimuth. Hamilton's equations of motion are numerically integrated to determine the positions and momenta of all the particles as a function of time. In previous simulations of both SIMS and ISS experiments we assumed that all the particles simultaneously interact via a sum of pairwise additive potentials [8,9]. In a separate study we have found that identical results for ISS trajectories can be obtained by neglecting the interactions among the metal atoms [10]. Therefore, the only interactions assumed in the calculations presented here are those between the incident particle and the substrate atoms. The primary particle, however, is allowed to interact simultaneously with all of the substrate atoms. This procedure is in contrast to most ISS simulations where only binary collisions are considered [1a–1c,4–6,11–13]. In all the simulations the particles obey the classical laws of motion regardless of whether the equations of motion are numerically integrated or whether deflection functions are used to propagate the ion's trajectory. The essential difference between our method and most others is the nature of the forces among the atoms.

A Molière potential was used to describe the interaction between the primary particle and the Rh atoms [14]. We found no basis for adjusting the Thomas–Fermi screening radius as has been done by other researchers [4,6,11,12]. In order to make a reasonable attempt at fitting this parameter more detailed experimental data are needed [15]. As discussed below the scattered ion intensity for He^+, Ne^+ and Ar^+ primary ions correlates well with

incident particle velocity. In principle, there could also have been effects due to the mass or size of the various incident ions. To eliminate all factors except the incident particle velocity, we have chosen to perform calculations for only Ne^+ particles incident at a polar angle of $\psi_{in} = 70°$ in both the $\langle 110 \rangle$ and $\langle 211 \rangle$ azimuths. The Ne^+ primary ion kinetic energy is varied between 0.5 and 6.0 keV. There are two distinct $\langle 211 \rangle$ directions ($\phi = \pm 30°$ of fig. 1b). As discussed in section 4, at an incident angle of 70° in the $\langle 211 \rangle$ direction, the second and third layer atoms are almost completely shadowed, and the $\phi = 30°$ and $\phi = -30°$ directions yield equivalent scattered distributions.

The primary particle must uniformly strike all points on the surface to reproduce the experimental conditions. From symmetry considerations, it is possible to represent the infinite {111} surface with the shaded hexagon shown in fig. 1b. For bombardment along the $\langle 211 \rangle$ azimuth this region may be cut in half due to the presence of a mirror plane of symmetry. Note that the placement of the second and third layer atoms breaks the mirror plane along the $\langle 110 \rangle$ direction. It is important to utilize a microcrystallite that is large enough to contain all the important scattering processes. This is particularly critical for these calculations since the primary ion is incident at nearly grazing angles which results in a multitude of different inplane scattering mechanisms [16]. In the $\langle 110 \rangle$ azimuth, for example, there are a series of zig-zag collisions which occur as the ion moves sideways through a channel created by two rows of surface atoms. The fact that these collisions occur across a long distance implies that relatively large crystals are needed. Careful testing has shown that at least two atomic rows are needed on each side of the impact zone (i.e. a total of five atom rows altogether) and that second and third layer atoms are required. Further, a surface length of 50–100 Å for 1.0 to 6.0 keV primary ion energies is needed. In the $\langle 211 \rangle$ direction a crystal with only the surface layer is sufficient to describe the vast majority of the collision processes since first layer scattering is most important. Since there are no long range zig-zag mechanisms in this crystal direction, a length of 15–25 Å and a width of ~ 5 Å is an adequate size needed to obtain reliable results.

For each set of initial conditions (Ne^+ energy, polar angle and azimuthal direction) $\sim 10^4$ collision sequences are calculated with the incident ion aimed randomly within the hexagonal surface region of fig. 1b. For each collision sequence that results in reflection from the surface, the initial conditions, final energy and angles, collision time and maximum depth of penetration in the solid are stored for subsequent analysis. Various graphical displays including energy distributions, polar angle distributions and contour plots are used to obtain a detailed understanding of the data. In addition specific trajectories of interest may then be recalculated in order to trace the important microscopic collision events.

4. Results

A typical azimuthal scan measured for 1.0 keV Ar^+ ions scattered from the clean Rh{111} surface is shown in fig. 2a. The scattered ion intensity exhibits considerable anisotropy with the maximum intensity observed in the ⟨211⟩ directions. It is not possible to determine whether the distribution is three-fold or six-fold symmetric since limitations in the experimental setup prevented full 360° scans. A three-fold symmetric pattern would indicate that there is a significant contribution to the yield from scattering from second and/or third layer atoms. The azimuthal scan obtained for 1.0 keV He^+ ions scattered from the clean Rh{111} surface is shown in fig. 2b. Anisotropy in the scattered ion intensity is also observed, although the yield is peaked in the ⟨110⟩ direction and the magnitude of the anisotropy is less. As a starting point in correlating all the experimental data, we chose to plot the ratio of the yield in the ⟨110⟩ direction to the yield in the ⟨211⟩ direction as a function of the velocity, v, of the incident ion (fig. 3a). An examination of the Molière potentials used in the

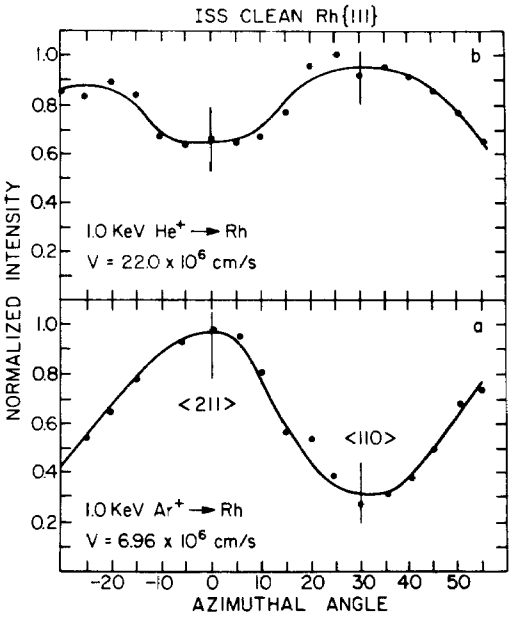

Fig. 2. Azimuthal scans of the scattered ion intensity for a primary ion energy of 1.0 keV. The polar angle of incidence is 70° and the collection angle is 60°. The intensities are measured at the peak in the energy distribution. The experimental peak shapes for different azimuths and energies are nearly identical, thus the peak intensities are proportional to the integrated intensities. The experimental peak position is within experimental uncertainty of the value predicted by the binary collision model. (a) Ar^+, (b) He^+.

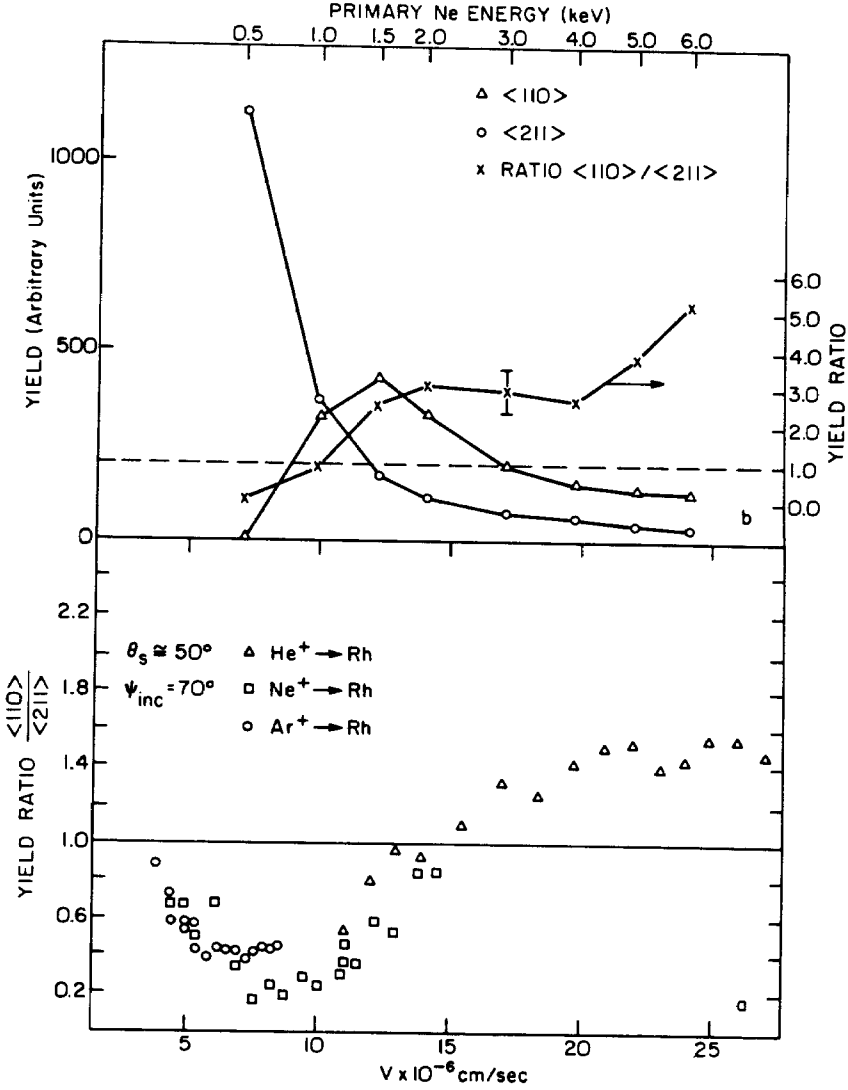

Fig. 3. The yield ratio as a function of velocity of the incident ion. In all cases only particles scattered inplane are counted. (a) Experimental results. (b) Calculated results for the total yield at $\psi_{ex} = 60 \pm 5°$. The Ne^+ kinetic energies are given at the top of the figure. The error bar represents one standard deviation.

calculation shows that an almost equivalent graph could have been generated by plotting the yield ratio versus the effective size of the atoms, a parameter which is particle type and energy dependent. Since the Molière potential is

approximately proportional to the atomic number and the energy to the mass, the velocity turns out to be closely related to the effective size of the atoms. Experimentally we find at low velocities the ratio is ~ 1 but rapidly decreases to a minimum of ~ 0.2 at ~ 8×10^6 cm/s. From this point the ratio increases approaching a limiting value of ~ 1.4 at ~ 25×10^6 cm/s. Despite the general velocity dependent trend observed, careful inspection of the He^+, Ne^+, and Ar^+ data points show a slight displacement of the individual values.

In order to understand the velocity dependence of the yield ratio, calculations are performed for Ne^+ scattering inplane from Rh{111} in the ⟨110⟩ and ⟨211⟩ directions. The calculated total yield at $\psi_{ex} = 60 \pm 5°$ for each direction as well as the yield ratio are given in fig. 3b for Ne at incident energies between 0.5 and 6.0 keV. Over this energy range, the calculations appear to reproduce, at least qualitatively, the experimental observations. To understand the factors that influence the magnitude of the yield ratio, the important microscopic mechanisms that contribute to the scattering intensities in each direction need to be analyzed in detail.

The calculated ⟨211⟩ yield for all the inplane scattered Ne particles is qualitatively the simplest to understand. For a primary ion angle of incidence of 70° from the surface normal, the second and third layer atoms are almost completely shadowed by the first layer atoms (fig. 1c). Thus, the yield is composed of scattering primarily from the first layer. The decrease in the ⟨211⟩ yield is due to the lower cross section for inplane collisions as the primary ion energy increases. The first layer mechanisms include the so called single and double scattering along the ridge of surface atoms as well as zig-zag collisions between two adjacent surface rows. The sharp drop in the ⟨211⟩ Ne yield from 0.5 to 1.0 keV is due primarily to a loss of yield of zig-zag collisions. The small decline in intensity between 4.0 and 5.0 keV is due to a loss of the inplane double scattering mechanism. This barely perceptible change in yield is the main factor responsible for the increase in the yield ratio from 4 to 6 keV.

In the ⟨110⟩ direction for energies above 1.5 keV, the yield exhibits a similar decrease in intensity as the primary ion energy increases. As seen from fig. 1d there are open channels between the first layer rows of atoms in the ⟨110⟩ direction. Thus, scattering from second and third layer atoms contributes to the yield of the ⟨110⟩ direction making it larger than the yield in the ⟨211⟩ direction at high velocities. In contrast to the ⟨211⟩ results there is a decrease in yield as the energy is decreased from 1.5 keV. At a primary ion energy of 0.5 keV the Rh surface appears to the primary ion to be quite smooth in the ⟨110⟩ direction. Virtually all of the particles scatter at a polar angle of ~ 70° (nearly specular). Although the total intensity of reflected ions is large, none are detected at $60 \pm 5°$. As the energy increases, the surface appears rougher to the primary ion and the polar angle distribution splits into two peaks at the minimum and maximum scattering angles [6]. The peak at ~ 70° is at the minimum total scattering angle and corresponds to quasi-double

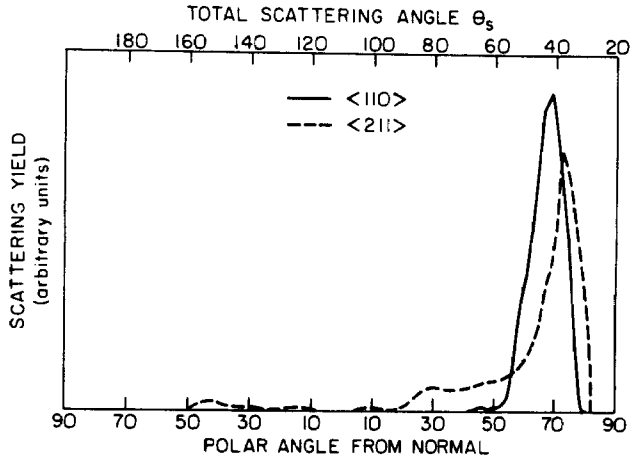

Fig. 4. Calculated polar angle distributions for inplane scattering of 1.5 keV incident Ne^+ ions incident at 70° from the surface normal.

scattering [17]. The position of this peak is relatively insensitive to the energy of the incident ion [6]. The peak at the maximum total scattering angle (more toward the surface normal) is due to single scattering [17] and is energy dependent [6]. As the primary ion energy increases this peak occurs at angles closer to the surface normal. The polar angle distribution for 1.5 keV incident ions is shown in fig. 4. One peak in the scattered intensity in the ⟨110⟩ direction is at 70° from the surface normal and a second peak appears as a shoulder at ~ 60° from the normal. As the energy increases further the second peak moves toward the surface normal. The increase in intensity in the ⟨110⟩ yield, then, from 0.5 to 1.5 keV occurs as this second peak passes through the polar angle range seen by the detector. Note that the ⟨211⟩ direction is rougher due to the larger spacing between atoms which results in a wider polar angle distribution (fig. 4). This is a subtle effect which dominates the experimental results and which would be difficult to elucidate without performing computer simulations. It should be noted that although the experimental yield is very low at a Ne^+ ion energy of 0.5 keV, it is not zero.

The calculated ratios of the ⟨110⟩ to the ⟨211⟩ yields are shown in fig. 3b. The qualitative features of the experimental results are reproduced. That is, at $v \approx 5 \times 10^6$ cm/s the ratio is small because particles incident in the ⟨110⟩ direction are not scattered into the detector at 60°. For large velocities subsurface scattering occurs in the ⟨110⟩ direction whereas the second and third layer atoms are almost completely shadowed in the ⟨211⟩ direction. In addition, due to the larger spacing between atoms in the ⟨211⟩ direction, there is a smaller contribution from first layer double scattering.

There are still discrepancies between the calculated and experimental ratios.

The experimental velocity at which the ratio is unity is larger than the calculated one. The experimental ratio at high velocities is equal to ~ 1.4 but is equal to ~ 5 in the calculations. There is an increase in the experimental ratio as very low velocities are approached. One obvious omission from the calculation is the effect of neutralization on the Ne^+ ion intensity. We have tried to account for neutralization by filtering out the collision events that take longer times [9]. This enhances single- and to some extent double-scattering from the first layer while suppressing the importance of zig-zag collisions and those which involve deeper layers. Some improvement is achieved in the yield ratio curve by applying this correction. The value of the ratio at high velocities can be decreased to ~ 1.5, although the ratio at 1.5–2.0 keV is still too high. Note that a neutralization probability that only depends on the velocity or its perpendicular component [18] will not substantially alter the yield ratio curve.

There is a peculiarity of this experimental geometry that makes it difficult to model. The collection angle is near the peak intensity of the polar angle distribution. The precise angle and resolution of collection is critical. From fig. 4 it is obvious that changing the collection angle in the region of 50–70° will alter the ratio of the yield in the two directions. We can obtain a better fit to the experimental yield ratio curve by slightly decreasing the polar angle of detection with respect to the normal and by decreasing the resolution. Since the experimental values are not known exactly, it is, then, difficult to make a precise comparison. Another uncertainty is the interaction potential. If the effective size of the atoms is decreased, then the surface roughness increases. This will alter the polar angle distribution as discussed above, especially in the region near 60°. Also omitted in the calculations are thermal motions of the Rh atom. The thermal effects will undoubtedly broaden the peaks in the polar distribution, but given the uncertainties discussed above, we do not feel that their inclusion would add insight into the process. On the other hand, the scattered ion intensity in this polar angle regime is high and one does not have to collect as much data to get statistically meaningful results either in the experiment or the calculations.

The remaining region of the yield curve that needs explanation is at low velocities where the yield ratio is ~ 1. The experimental intensities are much lower in this regime than at higher velocities. Our initial assumption was that at low primary ion velocities the Rh{111} surface should be smooth in both the ⟨110⟩ and ⟨211⟩ directions, and that the scattering would be isotropic. Attempts to confirm this with calculations of Ar^+ ion scattering at 500, 100 and 10 eV were unsuccessful. The ⟨211⟩ direction appears quite smooth as is indicated by almost 100% reflection of the incident Ar particles near the specular angle. In the ⟨110⟩ direction, however, the roughness between the two rows of first layer atoms continues to cause considerable out-of-plane scattering. It is unclear, then, what the reason is for the isotropic scattering at small velocities.

In contrast to the large anisotropies observed for $\psi_{in} = 70°$ and $\psi_{ex} = 60°$, for $\psi_{in} = 60°$ and $\psi_{ex} = 70°$ the scattered yields are nearly isotropic for both Ne^+ and He^+ ion scattering (velocities from 7 to 30×10^6 cm/s). The actual yield ratio is ~ 1.1 for all velocities, indicating slightly more reflection in the ⟨110⟩ direction. However, for Ne^+ scatterng from Ni{111} at energies between 0.2 and 0.4 keV, the same measured yield ratio is ~ 0.7 [6]. Thus only a slight change in the experimental conditions from that described above produces a very different azimuthal anisotropy (or lack of it). In this case the computer simulations are necessary to explain the observed intensities. Even though qualitative agreement is obtained between the experimental and calculated yield ratios without invoking neutralization, to obtain a better agreement one needs a realistic procedure for including this process. A neutralization probability that includes details of the collision process is required [2,9,19,20].

5. Conclusions

Angle-resolved ISS experiments have been performed for He^+, Ne^+ and Ar^+ scattering from Rh{111}. For an incident angle of 70° and a collection angle of 60°, both measured with respect to the surface normal, it is found that the scattered ion intensity is azimuthally anisotropic and that the direction of the peak intensity differs for the various ions. There is excellent correlation of the ratio of the yield in the ⟨110⟩ direction to the yield in the ⟨211⟩ direction with the incident particle velocity. The experimental ratio is ~ 1 at low velocities (~ 4×10^6 cm/s), decreases to ~ 0.2 at 8×10^6 cm/s and increases to a value of 1.4 at 25×10^6 cm/s.

Molecular dynamics calculations are reported for Ne^+ scattering with the same configurations as the experimental ones. We find qualitative agreement with the experimental results without having to account for neutralization effects. The small anisotropy ratio at 8×10^6 cm/s is due to lack of scattering of particles into the detector at $\psi_{ex} = 60°$ in the ⟨110⟩ direction. At the higher velocities, the second and third layer atoms are significantly shadowed in the ⟨211⟩ direction; consequently the yield in this direction is lower than in the ⟨110⟩ direction. In addition, the large spacing between atoms in the ⟨211⟩ direction reduces the contribution from double scattering along the chain of atoms. Improvement between the calculated yield ratios and the experimental values can be obtained if a neutralization probability that depends on the time the ion interacts with the solid is used.

In order to understand the spectrum of ion scattering from a clean unreconstructed Rh{111} metal surface, it was necessary to perform computer simulations. To be able to use geometrical arguments of channeling and blocking to interpret ISS spectra extreme care must be taken in choosing the experimental energies and angles of incidence and detection [1d,1e]. However, many ISS

experiments are not designed in this manner, and in these cases computer simulations provide a necessary aid for data interpretation and possible surface structure determination. Of particular note is that the anisotropy in this case reverses for velocities $\leqslant 15 \times 10^6$ cm/s. This result suggests that even if the experimental geometry was optimally chosen, interpretation of the scattering data in the low velocity regime might not be simple.

Acknowledgments

The financial support of the National Science Foundation, the Office of Naval Research, the Air Force Office of Scientific Research and the Petroleum Research Foundation administered by the American Chemical Society is gratefully acknowledged. One of us (B.J.G.) also thanks the Alfred P. Sloan Foundation for a Research Fellowship and the Camille and Henry Dreyfus Foundation for a grant for newly appointed young faculty and a Teacher–Scholar Award. We thank R. Blumenthal and S. Williams for helpful discussions and comments on the manuscript.

References

[1] See for example, (a) W. Heiland, Appl. Surface Sci. 13 (1982) 282;
(b) R.P.N. Bronckers and A.G.J. de Wit, Surface Sci. 104 (1981) 384;
(c) R.P.N. Bronckers and A.G.J. de Wit, Surface Sci. 112 (1982) 111 and 133;
(d) M. Aono, Y. Hou, C. Oshima and Y. Ishizawa, Phys. Rev. Letters 49 (1982) 567; 51 (1983) 801;
(e) R.S. Williams, J. Vacuum Sci. Technol. 20 (1982) 770.
[2] D.P. Woodruff and D.J. Godfrey, Solid State Commun. 34 (1980) 679; Surface Sci. 105 (1981) 438 and 459.
[3] E. Taglauer, W. Englert, W. Heiland and D.P. Jackman, Phys. Rev. Letters 45 (1980) 740.
[4] T.M. Buck, I. Stensgaard, G.H. Wheatley and L. Marchut, Nucl. Instr. Methods 170 (1980) 519.
[5] S.H. Overbury, W. Heiland, D.M. Zehner, S. Datz and R.S. Thoe, Surface Sci. 112 (1982) 23.
[6] W. Heiland, E. Taglauer and M.T. Robinson, Nucl. Instr. Methods 132 (1976) 655.
[7] L.A. DeLouise and N. Winograd, Surface Sci. 138 (1984) 417.
[8] K.E. Foley and B.J. Garrison, J. Chem. Phys. 72 (1980) 1018;
B.J. Garrison and N. Winograd, Science 216 (1982) 805.
[9] B.J. Garrison, Surface Sci. 87 (1979) 683.
[10] C.-C. Chang, B.J. Garrison and N. Winograd, unpublished results.
[11] D.P. Jackson, W. Heiland and E. Taglauer, Phys. Rev. B24 (1981) 4198.
[12] J.A. Yarmoff and R.S. Williams, Surface Sci. 127 (1983) 461.
[13] H.F. Helbig, M.W. Linder, G.A. Morris and S.A. Steward, Surface Sci. 114 (1982) 251.
[14] I.M. Torrens, Interatomic Potentials (Academic Press, New York, 1972).
[15] For example, polar distributions at a variety of incident angles and energies, H.B. Nielsen and T.A. Delchar, Surface Sci. 141 (1984) 487.
[16] Similar trajectories are shown for Na^+ ion scattering from Pt{111} in:
H. Niehus and E. Preuss, Surface Sci. 119 (1982) 349.

[17] B. Poelsema, L.K. Verhey and A.L. Boers, Surface Sci. 56 (1976) 445.
[18] H.D. Hagstrum, in: Electron and Ion Spectroscopy of Solids, Eds. L. Fiermans, J. Vennik and W. Dekeyser (Plenum, New York, 1978).
[19] E. Preuss, Surface Sci. 110 (1981) 287.
[20] J.N.M. van Wunnik, R. Brako, K. Makoshi and D.M. Newns, Surface Sci. 126 (1983) 618.